Agricultural Water Management 295 (2024) 108756

Contents lists available at ScienceDirect

Agricultural Water Management

journal homepage: www.elsevier.com/locate/agwat

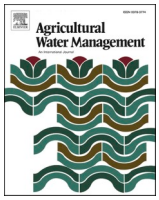

Influence of soil hydraulic parameters on bulb size for surface and buried emitters

Giorgio Baiamonte *, Vincenzo Alagna, Dario Autovino, Massimo Iovino, Samuel Palermo, Girolamo Vaccaro, Vincenzo Bagarello

Dept. of Agricultural, Food and Forest Sciences (SAAF), Univ. of Palermo, viale delle Scienze, Bldg. 4, Palermo 90128, Italy

ARTICLE INFO

Handling Editor - J.E. Fernández

Keywords:
Wetting bulb
Drip irrigation systems
Buried sources
Surface sources
Soil spatial variability
Philip's model

ABSTRACT

Predicting the size expansion of wetting bulbs during surface and subsurface drip irrigation is compulsory for water saving and helps drive irrigation design and scheduling. To solve these issues, various numerical and analytical models, which take into account for the soil hydraulic parameters have been suggested in the literature. The model introduced by Philip (1984) is based on closed-form dimensionless solutions to determine the vertical and horizontal dimensions of the bulb expansion for both buried and surface point sources, under the assumption of homogeneous soil hydraulic properties. In this paper, the solutions provided by Philip (1984) were reformulated in dimensional terms and applied to an already available large data set of soil hydraulic parameters measured in a citrus orchard to evaluate the impact of soil hydraulic properties variability on the development of the wetting front. The results showed that the range of variability of the bulb geometric variables is similar for both buried and surface sources, with a slightly smaller boundary width observed for surface versus buried emitters. More importantly, the geometric bulb variables corresponding to the soil dataset, which characterizes the same soil, turned out to be very different, demonstrating that the soil hydraulic parameters have a strong control over the bulb size. In particular, the soil hydraulic properties have an important effect on the downward vertical expansion of the bulb for both surface (CV = 15.5 %) and buried (CV = 18.5 %) point sources. While the horizontal expansion of the bulb from the surface source (CV = 10.6 %) and the upward vertical expansion from the buried source (CV = 12.7 %) are a bit less affected. Therefore, the risk of an inadequate soil hydraulic characterization could be an incorrect estimate of the irrigation volume to be imposed, thus underwatering or overwatering the root zone.

1. Introduction

Among the different irrigation methods, drip irrigation represents the most efficient system to satisfy the crop water demand while maintaining high yield rates (Baiamonte, 2016; Provenzano et al., 2016). The high efficiency of drip irrigation systems is related to the small volume of the wetted soil compared to the entire volume of soil (Goyal, 2014). If well designed, the system can achieve values of water use efficiency well above 90 % (Autovino et al., 2016).

Besides the correct design, it is important that the irrigation system is correctly managed (Barragan et al., 2010). Autovino et al. (2016) proposed a methodology to evaluate the optimal irrigation volume of a crop based on the crop production function, field distribution uniformity and economic evaluations. This approach, however, does not consider the spatial variability of soil hydraulic properties.

Knowledge of water dynamics during drip irrigation is of crucial importance for the design of efficient systems. The wet bulb should develop just in the zone where the active roots are present, thus enhancing root water uptake and reducing water losses by evaporation or percolation (Fernández-Gálvez and Simmonds, 2006; Kandelous and Šimůnek, 2010a, 2010b; Subbaiah, 2013). Reaching this issue is necessary to maximize water use efficiency, thus saving water in agriculture management contexts. Moreover, predicting bulb size is expected to allow for appropriate choices concerning subsurface emitters' depth, and emitters' spacing.

The lateral movement of water away from a dripper, compared to its depth of penetration, is determined by the relative importance of the soil hydraulic conductivity and sorptivity (Revol et al., 1997). It is widely recognized that the volume of the bulb, its shape, and the spatial distribution of soil moisture under micro-irrigation vary with irrigation volume and soil hydraulic properties (Lafolie et al., 1989; Lubana et al.,

* Corresponding author.
E-mail address: giorgio.baiamonte@unipa.it (G. Baiamonte).

https://doi.org/10.1016/j.agwat.2024.108756
Received 7 August 2023; Received in revised form 20 February 2024; Accepted 27 February 2024
Available online 2 March 2024

Nomenclature

$(s_0)_{surface}$	Horizontal expansion of the bulb for surface point sources (cm)
$(z_{up}+z_{dn})_{buried}$	Total vertical bulb length for the buried source (cm)
$(z_{dn})_{buried}$	Vertical downward bulb dimension for buried point sources (cm)
$(z_{dn})_{surface}$	Vertical downward bulb dimension of the bulb for surface point sources (cm)
$(z_{dn})_{surface}/(s_0)_{surface}$	Bulb shape index for surface point sources (cm)
$(z_{up})_{buried}$	Vertical upward bulb dimension for buried point sources (cm)
$\overline{\theta}$	Difference between θ_{av} and θ_s ($cm^3\ cm^{-3}$)
A	Constant of Haverkamp's model (mm^{-1})
b	Capillary scale parameter (dimensonless)
b_s	Intercept of the straight line fitted to the data describing steady-state conditions on the I vs. t plot (mm)
C	Constant of Haverkamp's model (dimensonless)
CV	Coefficients of variation (%)
D	Diameter of the ring used on beerkan runs (m)
h	Soil water pressure head (m)
I	Cumulative infiltration of the water in the soil (mm)
i_s	Slope of the straight line fitted to the data describing steady-state conditions on the I vs. t plot ($mm\ h^{-1}$)
K	Soil hydraulic conductivity ($mm\ h^{-1}$)
K_i	Initial soil hydraulic conductivity ($mm\ h^{-1}$)
K_s	Saturated soil hydraulic conductivity ($mm\ h^{-1}$)
P	Probability value (dimensonless)
q	Source strength i.e. emitter flow rate ($L\ h^{-1}$)
r	Radius of the infiltration surface (mm)
R	Polar distance from the point source (cm)
ϕ	Angle from the polar direction (rad)
R^2	Coefficient of determination (dimensonless)
S	Soil sorptivity ($mm\ h^{-0.5}$)
S_0	Dimensionless horizontal bulb expansion from surface sources (dimensonless)
s_0	Bulb horizontal expansion from surface point sources (cm)
t	Time (h)
T	Dimensionless travel time of marked particles (dimensonless)
V	Water volume applied by the emitter (L)
w_i	Initial gravimetric soil water content ($g\ g^{-1}$)
z_{dn}	Dimensional downward bulb size for the buried and the surface sources (cm)
Z_{dn}	Dimensionless downward bulb size for the buried and the surface sources (dimensonless)
z_e	Burial depth of the emitter (cm)
z_{up}	Dimensional vertical upward bulb size for buried point sources (cm)
Z_{up}	Dimensionless vertical upward bulb size for buried point sources (dimensonless)
ΔK	Difference between K_s and K_i ($mm\ h^{-1}$)
$\Delta\theta$	Difference between θ_s and θ_i ($cm^3\ cm^{-3}$)
α	Parameter of the Gardner's hydraulic conductivity function (m^{-1})
β	Shape constant of Haverkamp's model (dimensonless)
γ	Correction constant of Haverkamp's model (dimensonless)
λ_c	Macroscopic capillary length (mm)
θ_{av}	Average volumetric soil water content behind the wetting front ($cm^3\ cm^{-3}$)
θ_i	Initial volumetric water content prior to wetting ($cm^3\ cm^{-3}$)
θ_s	Saturated volumetric soil water content ($cm^3\ cm^{-3}$)
ρ_b	Dry soil bulk density ($g\ cm^{-3}$)

2004). Therefore, the ability to predict the size of the wetted bulb is important, both to ensure efficient irrigation and to avoid the environmentally deleterious drainage of irrigation water below the root zone (Nakayama and Bucks, 1986; Keller and Bliesner, 1990). Since the exact wetting pattern and moisture distribution depend on many factors, including initial soil conditions, emitter flow rate, irrigation volume, frequency and root distribution pattern, different methods to estimate the wetted bulb size were developed (Subbaiah, 2013).

The wetting pattern can be obtained through direct measurements or estimated by infiltration models. To estimate the wetting front distance from a surface or subsurface dripper, several approaches have been proposed that rely on empirical, analytical, or numerical models (Lubana and Narda, 2001).

The empirical models are developed from regression analysis, dimensional analysis an artificial neural network (Singh et al., 2006). These models are simple and do not need specific knowledge of the soil hydraulic properties. However, the reliability of the results is strongly affected by the dataset used for their calibration/validation process. As a consequence, their use for soils different from those for which the models have been developed should be conducted with caution.

The analytical models allow determining the horizontal and vertical dimensions of the wetting pattern through a solution of differential equations generally derived under simplified assumptions for the geometry and the initial and boundary flow conditions (Subbaiah, 2013). The strength of these models is represented by their relative simplicity of use associated to accurate solutions. Subbaiah (2013) defined the analytical models as "irreplaceable" since they can provide a direct insight into the physics of unsaturated flow, especially when dealing with the effects of several parameters.

The numerical models are based on the solution of the Richards (1931) equation. Unlike empirical or analytical models (Broadbridge et al., 2017; Baiamonte et al., 2023), they offer greater flexibility thus allowing a realistic simulation of natural flow systems under different initial conditions and imposed boundary constraints. However, numerical models require a detailed knowledge of the soil hydraulic properties of soils, expertise and experience in use and can be computationally intensive.

Philip (1984) provided a closed-form dimensionless solution in spherical polar coordinates for the travel time of a marked particle emitted from a buried infiltration point source and a surface point source. Several authors have applied different models to study the effect of emitter discharge rate, initial soil moisture and soil texture on the size of the wetting pattern (Ayers and Westcot, 1985; Thorburn et al., 2003; Al-Ogaidi et al., 2016). These studies are based on the assumption of homogeneous soil with uniform initial moisture content. However, due to structural heterogeneities (i.e., biological and structural macropores, cracks), the soil hydraulic properties exhibit both small- and large-scale spatial variability that may influence the wetted bulb size (Warrick, 1998). Regalado and Muñoz-Carpena (2004) investigated the spatial variability of the saturated hydraulic conductivity, K_s, of a drip irrigated volcanic soil. Depending on the measurement method (laboratory, Guelph and Philip-Dunne permeameters) and the flow dimensionality, coefficients of variation (CV) from 5.7 % to 72.4 % for saturated hydraulic conductivity were detected. Due to the spatial variability within a field, simulation of a single mean wetting pattern for drip irrigation may not be sufficient to design an irrigation system efficiently. For this reason, when designing a localized irrigation system, it is important not only to know the average soil hydrodynamic properties but also their variability. Several spatial variability studies of saturated and unsaturated hydraulic conductivities of agricultural soils have been conducted

by different researchers (e.g., Das Gupta et al., 2006), while the influence of the spatial variability of soil hydraulic properties on the water dynamics during drip irrigation has been poorly addressed. The BEST (Beerkan Estimation of Soil Transfer parameters) procedure of soil hydraulic characterization (Lassabatère et al., 2006) appears a good candidate method to simply describe variability of soil hydrodynamic properties in drip irrigated soils (Mubarak et al., 2009). This topic is of great relevance because neglecting or improperly considering the influence of the soil hydraulic characteristics in irrigation management, can negatively affect water saving, which deserves more and more attention in the next few years.

This study aimed at assessing the impact of soil hydraulic properties on predicting infiltration and wetting front from point sources located both on the soil surface and buried into the soil. By using an already available large data set of soil hydraulic parameters measured in an untilled and no-trafficked citrus orchard (Typic Rhodoxeralf), where the soil was classified as mostly sandy-loam or loam, the impact of the range of variability of the soil hydraulic properties on the development of the wetting front was investigated. Soil variability effects on the bulb geometric variables, for both buried and surface point sources, were also analysed.

2. Theoretical background

2.1. Soil hydraulic characterization

The cumulative infiltration curve obtained by a beerkan run, which consists in repeatedly applying a fixed and small water volume on the soil surface and recording the infiltration time of each water volume, can be used to determine the soil hydraulic properties by the so-called BEST procedure of soil hydraulic characterization (Lassabatère et al., 2006). In particular, the BEST-steady algorithm yields and estimate of soil sorptivity, S (mm $h^{-0.5}$), and saturated soil hydraulic conductivity, K_s (mm h^{-1}), using the intercept, b_s (mm), and the slope, i_s (mm h^{-1}), of the straight line fitted to the data that describe steady-state conditions on the cumulative infiltration, I (mm), versus time, t (h), plot (Bagarello et al., 2014):

$$S = \sqrt{\frac{i_s}{A + \frac{C}{b_s}}} \tag{1}$$

$$K_s = \frac{C\, i_s}{A\, b_s + C} \tag{2}$$

in which A (mm^{-1}) and C are constants that, for an antecedent volumetric soil water content, θ_i, less than 0.25 times the volumetric water content of the saturated soil, θ_s, can be set at (Haverkamp et al., 1994; Lassabatère et al., 2006):

$$A = \frac{\gamma}{r\,\Delta\theta} \tag{3a}$$

$$C \approx \frac{1}{2(1-\beta)} \ln\left(\frac{1}{\beta}\right) \tag{3b}$$

where $\Delta\theta$ is θ_s - θ_i, r (mm) is the radius of the infiltration surface and γ and β are coefficients commonly assumed equal to 0.75 and 0.6, respectively.

The macroscopic capillary length, λ_c (mm), that expresses the relative importance of capillarity over gravity forces during water movement in unsaturated soil, is given by White and Sully (1987):

$$\lambda_c = \frac{b\, S^2}{\Delta\theta\, \Delta K} \tag{4}$$

where b is a dimensionless capillary scale parameter frequently set equal to 0.55 and ΔK is the difference between K_s and the initial soil hydraulic conductivity, K_i (mm h^{-1}). Low λ_c values (e.g., $0 < \lambda_c \leq 10$ mm) indicate a dominance of gravity over capillarity and are typically found in coarse-textured or highly structured porous media. Instead, high λ_c values (i.e., >1000 mm) indicate the dominance of capillarity over gravity, as found in many fine-textured or poorly structured porous media. According to Di Prima et al. (2020), λ_c can be obtained from a steady-state beerkan infiltration run as follows:

$$\lambda_c = 0.861 \frac{b_s}{\Delta\theta} \tag{5}$$

2.2. Wetting patterns for surface and subsurface drip irrigation

Under the assumption of homogeneous soil hydraulic properties, for buried and surface infiltration point sources, Philip (1984) provided closed-form dimensionless solutions for the travel times of marked particles. For particular cases of the considered spherical polar coordinates (R, ϕ) (Fig. 1), $\phi = 0$, π (vertical direction) and $\phi = \pi/2$ (horizontal direction), these solutions are very simple, and although implicit with respect to the geometric variables denoting the size of the expanding bulb, allow assessing the impact of soil hydraulic properties on the predicted infiltration and on the related wetting front advancement, which is compulsory for the appropriate design of drip irrigation systems.

For a buried (burial depth, $z_e > 0$) and a surface (burial depth, $z_e = 0$) point source, Fig. 1 shows a schematic representation of the bulb, where the geometric variables investigated in this work, vertical upward and downward, z_{up} (cm) and z_{dn} (cm), for buried source (Fig. 1a) and horizontal and downward, s_0 (cm) and z_{dn} (cm), for surface source (Fig. 1b), are indicated. For both cases, these geometric variables do not explore the entire bulb size. However, it is expected that they provide an exhaustive analysis of the effect of the variability of soil hydraulic parameters on the bulb expansion since it is possible to consider that all the other points belonging to the bulb have a similar behaviour.

In order to limit water losses, the design and management of a buried irrigation system must ensure that the value of z_{up} will not exceed the water line installation depth, while the sum of z_{dn} and z_e should not exceed the rooting depth. In the case of surface irrigation, it is important that the value of s_0 is as limited as possible to reduce the evaporating soil surface and, also in this case, that z_{dn} value should not exceed the rooting depth. On the other hand, low s_0 values could compromise the necessary overlap of the wetting bulb and the root zone. For this reason, the calculation of these four lengths will be treated in detail below.

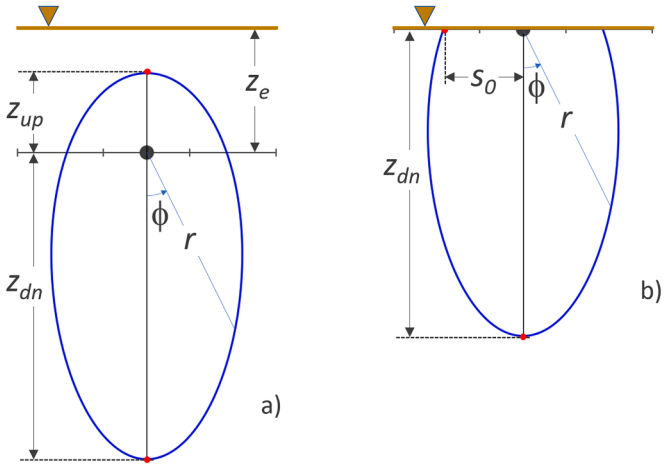

Fig. 1. Schematic representation of the bulb size from a) a buried point source (burial depth, $z_e > 0$) and b) a surface point source (burial depth, $z_e = 0$). The investigated variables z_{up} and z_{dn}, for the buried emitter (black dot), and s_0 and z_{dn}, for the surface emitter, are indicated.

2.2.1. Dimensionless parameters

According to Philip (1984), the dimensionless travel time T can be defined as:

$$T = \frac{\alpha^3 q\, t}{16\pi\, \overline{\theta}} \tag{6}$$

where α (m^{-1}) is the parameter of the exponential hydraulic conductivity function by Gardner (1958), q ($mm^3\ h^{-1}$) is the source strength, i.e. the emitter flow rate, t (h) is the irrigation time, V (L) is the water volume applied by the emitter, and $\overline{\theta} = \theta_{av} - \theta_i$, where θ_{av} ($cm^3\ cm^{-3}$) is the average volumetric water content in the soil behind the wetting front and θ_i ($cm^3\ cm^{-3}$) is the initial volumetric water content before wetting. In this investigation, θ_{av} was approximated as $(\theta_s+\theta_i)/2$. A certain approximation in the choice of the water contents to be used for calculating $\overline{\theta}$ was unavoidable, also considering that definitions do not seem univocal. For example, the water content at the wetting front was assumed as the θ value when K was equal to 1 mm day^{-1} by Cook et al. (2003) and 1 mm h^{-1} by Thorburn et al. (2003).

The α parameter in Eq. (6) is the slope of the ln K vs. soil water pressure head, h, relationship by Gardner (1958). For a Gardner soil (Youngs et al., 1993), α could potentially be estimated from the K values corresponding to any two values of h. In general, estimating α requires fitting the hydraulic conductivity model to a set of $K(h)$ data. Taking into account that, with drip irrigation, an initially nearly dry soil is wetted up to near saturation, the range of interest of h is rather wide, varying from very negative (dry soil) to little negative or nearly null (wetted soil) values. This circumstance has to be taken into account if λ_c is used to determine α (e.g., Thorburn et al., 2003) since α describes the entire hydraulic conductivity function but λ_c decreases as θ_i increases (White and Sully, 1987). Therefore, a determination of λ_c, and hence $\alpha = \lambda_c^{-1}$, performed in an initially wet soil can be expected to yield a different result than that of an experiment performed in an initially dry soil. In particular, a wet soil could yield a larger α value than a dry soil.

For both buried and surface sources, the dimensionless downward size, Z_{dn}, is denoted as (Fig. 1):

$$Z_{dn} = \frac{\alpha\, z_{dn}}{2} \tag{7}$$

whereas, for the buried and the surface sources, the dimensionless upward size and horizontal size are denoted, respectively:

$$Z_{up} = \frac{\alpha\, z_{up}}{2} \tag{8}$$

$$S_0 = \frac{\alpha\, s_0}{2} \tag{9}$$

where z_{up} (cm) and s_0 (cm) are the corresponding dimensional variables.

2.2.2. Dimensionless relationships

For a buried source, the dimensionless solutions of the wetting front travel-time provided by Philip (1984) are:

$$T = \frac{e^{2\, Z_{up}}\left(1 - 2\, Z_{up} + 2\, Z_{up}^2\right) - 1}{2} \tag{10}$$

$$T = \frac{\left(Z_{dn}^2 - Z_{dn}\right)}{2} + \frac{\log\left(1 + 2\, Z_{dn}\right)}{4} \tag{11}$$

whereas for a surface source the following relationships were derived (Philip, 1984):

$$T = \frac{Z_{dn}^2}{2} - Z_{dn} + \log(1 + Z_{dn}) \tag{12}$$

$$T = 2\, e^{S_0}\left(1 - S_0 + \frac{S_0^2}{2}\right) - 2 \tag{13}$$

2.2.3. Dimensional relationships

A great advantage of the above-mentioned dimensionless solutions derived by Philip (1984) lays in the reduced number of parameters contained in them. Therefore, it is easy to interpret the effect of proportional variations of one variable on the other.

For the purpose of this study, which aims at detecting the impact of the soil hydraulic parameters on bulb sizes, the same relationships reformulated in dimensional terms are necessary to investigate the impact of the soil hydraulic properties.

In particular, for the buried source, associated with Eq. (10) and Eq. (11), we obtain:

$$V = \frac{4\pi\, \overline{\theta}}{\alpha^3}\left[e^{\frac{\alpha\, z_{up}}{2}}\left(2 + \alpha\, z_{up}\left(\alpha\, z_{up} - 2\right)\right) - 2\right] \tag{14}$$

$$V = \frac{2\pi\, \overline{\theta}}{\alpha^3}\left[\alpha\, z_{dn}(\alpha\, z_{dn} - 2) + 2\log(1 + \alpha\, z_{dn})\right] \tag{15}$$

whereas for the surface source, associated with Eqs. (12) and (13), we derive:

$$V = \alpha^3\, \frac{2\pi\, \overline{\theta}}{\alpha^3}\left[\alpha\, z_{dn}(\alpha\, z_{dn} - 4) + 8\log\left(1 + \frac{\alpha\, z_{dn}}{2}\right)\right] \tag{16}$$

$$V = \frac{4\pi\, \overline{\theta}}{\alpha^3}\left[e^{\frac{\alpha\, s_0}{2}}\left(8 + \alpha\, s_0(\alpha\, s_0 - 4)\right) - 8\right] \tag{17}$$

The water volume applied by the emitter, V, was considered as a dependent variable, so that any combination of the emitter flow rate, q, and the irrigation time, t, can be explained by V.

The above dimensional relationships also allow practical applications, as determining the water volumes required to achieve an assigned vertical bulb length. For surface sources, Eq. (16) solves this issue, whereas for buried sources, Eqs. (14) and (15) need to be combined. Putting Eqs. (14) and (15) as equal yields:

$$\frac{4\pi\, \overline{\theta}}{\alpha^3}\left[e^{\frac{\alpha\, z_{up}}{2}}\left(2 + \alpha\, z_{up}\left(\alpha\, z_{up} - 2\right)\right) - 2\right] = \frac{2\pi\, \overline{\theta}}{\alpha^3}\left[\alpha\, z_{dn}(\alpha\, z_{dn} - 2) + 2\log(1 + \alpha\, z_{dn})\right] \tag{18}$$

From Eq. (18), an implicit equation linking z_{dn} and z_{up}, which does not depend on $\overline{\theta}$, can be derived:

$$z_{dn} = \frac{4 - 2\, e^{\alpha\, z_{up}\left(2 - \alpha\, z_{up}\left(2 - \alpha\, z_{up}\right)\right) + 2\log(1 + \alpha\, z_{dn})}}{\alpha\left(2 - \alpha\, z_{dn}\right)} \tag{19}$$

For a given water volume, V, Eq. (19) allows estimating the total vertical length for the buried source $(z_{up} + z_{dn})_{buried}$. Eq. (14) or Eq. (15) are used to determine z_{up} or z_{dn}. Then, Eq. (19) is solved for the other unknown variable (z_{dn} or z_{up}).

Applications of the above dimensional relationships take into account the influence of the soil hydraulic properties simply with the α parameter. Consequently, by applying the reformulated Philip's model it is possible to estimate the variability of the bulb expansion by having a dataset relating to the spatial variability of the α parameter which can be obtained with simplified approaches e.g. BEST procedures.

3. Materials and methods

The field experiment was performed at the Agricultural, Food and Forest Sciences Department of the University of Palermo (Italy), in a no-tilled and no-trafficked citrus orchard with trees spaced 4 m × 4 m apart (coordinates 33S 355511E 4218990N). The soil at the field site (Typic Rhodoxeralf) has a relatively high gravel content and it is mostly sandy-loam or loam down to a depth of at least 0.30 m. This soil has been chosen since it is representative of the agricultural area around Palermo city (Sicily) where the prevailing crop is citrus orchard mostly irrigated

with surface and subsurface drip irrigation systems. Data for this investigation were collected in an area of approximately 200 m^2, in which the soil had mainly a loam texture, according to the USDA classification system (clay = 15.4 %, silt = 36.2 %, sand = 48.4 %). The soil surface was gently levelled and smoothed by manual implements before sampling. To sample a bare area, the superficial herbaceous vegetation has been cut with a knife when it was present, while the roots remained in situ. Small diameter (D = 0.08 m) rings were inserted on the soil surface to a depth of 0.01 m for the beerkan infiltration runs. Ring insertion was conducted manually or by gently using a rubber hammer and ensuring that the upper rim of the ring remained horizontal during insertion.

A total of 56 beerkan runs were performed at randomly selected locations from May to July 2022. For each run, 20 water volumes, each of 57 mL, were successively poured, each in approximately 3 s, on the confined infiltration surface by applying water at a small distance from the infiltration surface, i.e. approximately at a height of 0.03 m. Therefore, a total of 227 mm of water were applied with a beerkan run. Water energy was dissipated on the fingers of the hand to minimize soil disturbance due to water application (Reynolds et al., 2002). For each water volume (1st, 2nd, …, 20th), the infiltration time was measured from water application to disappearance of all water, when the subsequent water volume was poured on the infiltration surface.

At the beginning of a working day, two undisturbed soil cores (0.05 m in height by 0.05 m in diameter) were collected in three different points of the area at the 0–0.05 m and 0.05–0.10 m depths. These cores were used to determine the dry soil bulk density, ρ_b, and the antecedent gravimetric soil water content, w_i, and hence θ_i. The means of the ρ_b and θ_i determinations were then associated with the beerkan runs performed on that day. Overall, 21 soil cores were collected for a given sampling depth. A two-tailed, paired t test was applied to compare the ρ_b and the w_i values obtained at the two depths.

The dataset used in this investigation was developed by re-analysing some of the infiltration curves obtained by Agosta et al. (2023). In particular, these authors performed three subsequent infiltration runs at a given sampling point during a nearly two-week period and they established comparisons between subsequent runs by considering the infiltration parameters of the Horton model (Horton, 1941). For each sampling point, only the first run was considered in this investigation since, in the other cases, the soil was initially too wet for applying BEST methods of data analysis (Lassabatère et al., 2006) or representative antecedent soil water content data were not collected and hence soil hydrodynamic parameters could not be calculated.

For each run, S, K_s and λ_c were calculated by Eqs. (1), (2) and (5), respectively. The normal distribution hypothesis of these data was then checked with the Lilliefors (1967) test. A regression analysis between two datasets was performed by considering the exponential, linear, logarithmic and power relationships and retaining the relationship having the highest coefficient of determination, R^2, for further analysis. A two-tailed t test was used to establish the statistical significance of a fitted regression line to the data (Glantz, 2012). All statistical tests were carried out at P = 0.05.

4. Results and discussions

4.1. Soil hydraulic characterization

The subsoil (5–10 cm) was less compacted and wetter than the upper soil layer (0–5 cm) (Table 1). However, both the ρ_b and the w_i values differed by only a little between the two sampling depths, that is by 0.07 g cm^{-3} and 0.03 g g^{-1}, respectively. Therefore, differences between the two soil layers were overall small. The θ_i/θ_s ratio, with θ_s estimated from the dry soil bulk density, varied between 0.10 and 0.21. Therefore, BEST calculations were possible since θ_i/θ_s was steadily smaller than 0.25 (Lassabatère et al., 2006). In this perspective, performing beerkan infiltration runs and using BEST methods to analyse the data seems appropriate to obtain usable λ_c values for bulb size prediction according to Philip (1984). The reason is that the infiltration experiment has to be performed in an initial nearly dry soil ($\theta_i \leq 0.25\ \theta_s$; Lassabatère et al., 2006) and it establishes saturated soil conditions close to the infiltration surface. This situation is similar to that realized by point source irrigation. In other words, the infiltration experiment characterizes a soil by considering a relevant range of θ values in the perspective to predict the size of the wetted bulb.

The hypothesis that S, K_s and λ_c were normally distributed was not rejected by the Lilliefors (1967) test. Consequently, the data were summarized by the arithmetic mean and the associated coefficient of variation, CV (Table 2). The S and K_s values were rather close to those previously obtained at the same field site and in the same period of the year by Bagarello et al. (2023). In particular, these last authors obtained a mean sorptivity of 126 mm $h^{-0.5}$ in May and of 160 mm $h^{-0.5}$ in July. These mean values differed at the most by 1.2 times from the mean S value obtained in this investigation. The corresponding means of K_s were equal to 194 and 158 mm h^{-1} and they differed at the most by 1.4 times from the results of this investigation. The similarity between the two investigations suggested that the developed dataset was representative enough of the field site for a nearly dry or rather dry soil. Moreover, the CV of K_s found in this investigation was very close to that (CV = 35.7 %) obtained by another BEST algorithm at the same site by Bagarello et al. (2014). However, variability of the soil hydrodynamic parameters should be expected to vary with several factors including the sampling period in the year. According to (Warrick, 1998), all soil hydrodynamic parameters obtained in this investigation exhibited a medium variation.

On average, capillarity was moderate since it was approximately equal to 90 mm (Table 2) and λ_c values of 42–125 mm are indicative of a moderate capillarity (Elrick and Reynolds, 1992; Di Prima et al., 2020). This capillarity category was detected at the 89 % of the 56 sampled points. In five cases, capillarity was strong but close to moderate since λ_c did not exceed 160 mm and strong conditions are expected for λ_c values

Table 2
Summary statistics of the soil hydrodynamic parameters (sample size, N = 56 for each parameter).

Parameter	Min	Max	Mean	CV (%)
S (mm $h^{-0.5}$)	57.5	207.1	128.7	25.0
K_s (mm h^{-1})	35.9	410.5	227.2	37.6
λ_c (mm)	12.4	157.7	89.6	33.1

Table 1
Summary of the dry soil bulk density, ρ_b, and antecedent gravimetric soil water content, w_i, values for the 0–5, 5–10 and 0–10 cm sampling depths obtained before the beerkan runs (sample size, N = 21 for each dataset) (adapted from Agosta et al., 2023).

Statistic	ρ_b (g cm^{-3})			w_i (g g^{-1})		
	0–5 cm	5–10 cm	0–10 cm	0–5 cm	5–10 cm	0–10 cm
Min	1.069	1.049	1.090	0.029	0.060	0.044
Max	1.303	1.185	1.222	0.117	0.122	0.120
Mean	1.175 a	1.107 b	1.141	0.053 a	0.086 b	0.070 a
CV (%)	5.0	3.2	3.3	44.2	23.4	30.3

ranging between 125 and 1000 mm. In a single case, capillarity was weak and close to negligible according to the ranges reported by Di Prima et al. (2020) since λ_c was equal to 12.4 mm and $\lambda_c \leq 10$ mm denotes a negligible capillarity.

Soil sorptivity increased with saturated soil hydraulic conductivity according to a statistically significant relationship ($R^2 = 0.50$, $R > 0$) (Fig. 2). This result was physically plausible taking into account that, according to Stewart et al. (2013), sorptivity also depends, in addition to soil capillarity representing the driving force, on soil hydraulic conductivity that expresses the dissipation. The relationships between λ_c and both K_s and S were weak ($R^2 = 0.13$ and 0.19, respectively) albeit statistically significant. In particular, λ_c decreased as K_s increased whereas an increase of S determined an increase of λ_c. Even these results were physically convincing since low λ_c values indicate a dominance of gravity over capillarity (e.g., Di Prima et al., 2020). This dominance is more and more expected as the soil becomes more conductive and less sorptive.

As shown in Fig. 2, the run yielding the lowest λ_c value (12.4 mm) deviated considerably from the other runs, despite the generally high data scattering. This particularly low λ_c value was obtained since the cumulative infiltration curve was nearly linear from the beginning of the run and hence the b_s intercept was small. A logical implication could be excluding this run from the subsequent analysis, considering the data obtained with this run as outliers. However, the shapes of infiltration curves can be highly variable, depending on many factors and processes (e.g., Angulo-Jaramillo et al., 2019), and Pachepsky and Karahan (2022) recently suggested that there are no reasons to assume that only concave and concave-to-linear cumulative infiltration curves can exist in nature. Moreover, BEST-steady yielded possible (i.e., positive) estimates of S and K_s and the calculated values of these two hydrodynamic parameters for this run did not deviate substantially from those obtained with the other runs (Fig. 2). In particular, $S = 58$ mm h$^{-0.5}$ and $K_s = 301$ mm h^{-1} were obtained for the run yielding the smallest λ_c value and, without this data point ($N = 55$), the calculated S and K_s values were in the range 58–207 mm h$^{-0.5}$ and 36–411 mm h^{-1}, respectively. Finally, λ_c was very low but physically possible (Di Prima et al., 2020). Therefore, there was not any strong reason to exclude this apparent outlier from the subsequent analysis.

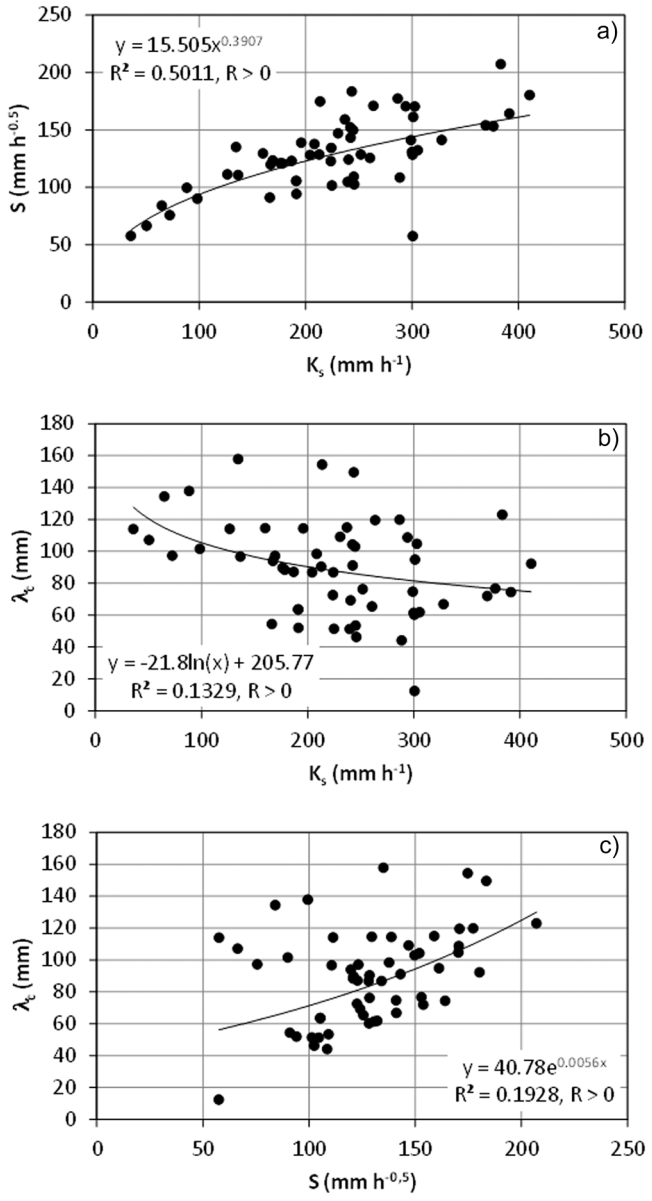

Fig. 2. Relationships between soil sorptivity, S, saturated hydraulic conductivity, K_s, and macroscopic capillary length, λ_c ($N = 56$).

4.2. Wetting patterns

For a reasonable value of the water volume applied by the emitter during one irrigation, $V = 10$ L, which could be ascribed to $q = 2.1$ L h^{-1} flow rate and 4.76 h of the irrigation time, Fig. 3 plots the frequency distribution of the studied variables, z_{up} and z_{dn} (Eqs. (18) and (19), for the buried source (dots), and s_0 and z_{dn} (Eqs. 20 and 21), for the surface source (circles), corresponding to the investigated dataset.

For both buried and surface sources, Fig. 3 shows that z_{up} and s_0 appear a little less influenced by the soil property variability, expressed by $\alpha^3/\overline{\theta}$, than z_{dn}, as quantified by the coefficient of variation CV that for buried sources equals $CV(z_{up}) = 12.7$ % and $CV(z_{dn}) = 18.5$ %, whereas for surface sources $CV(s_0) = 10.6$ % and $CV(z_{dn}) = 15.5$ %. Moreover, according to the α outlier (81 m^{-1}), $z_{dn} = 73.7$ cm and 74.7 cm, for buried and surface sources, respectively, occurred. The latter suggests that for high α, buried sources provide vertical bulbs that do not expand appreciably above the burial plane, contrary to what is observed in other cases.

Bulb sizes were investigated in some detail, by considering the 56 sampling points, each characterized by $\alpha^3/\overline{\theta}$. Taking into account that $\overline{\theta}$ varied only a little in this investigation ($N = 7$, mean = 0.246 cm^3 cm^{-3}; $CV = 4.3$ %), each sampling point was only characterized by its α value. Applications were performed by varying the irrigation volume, V (L), which depends on both the emitter flow rate and the irrigation time.

For the entire dataset, Eqs. (18) and (19), for a buried source, and Eqs. (20) and (21), for a surface source, were log-log plotted against α for different V values (5, 10, 20, and 30 L) in Fig. 4a and b, respectively.

For the considered soil and for any V, Fig. 4 shows that, for a buried

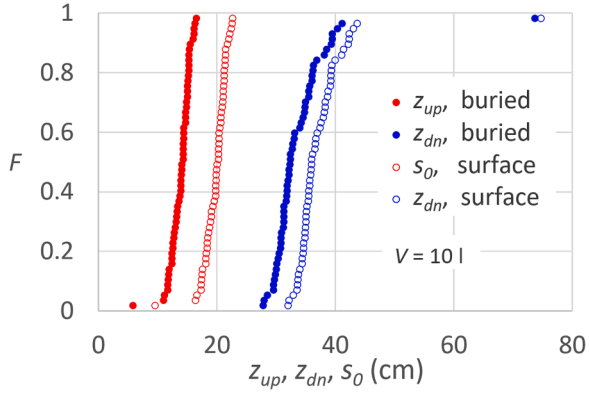

Fig. 3. For the considered dataset, and for $V = 10$ l, frequency distribution of z_{up} and z_{dn}, for the buried source, and of s_0 and z_{dn}, for the surface source.

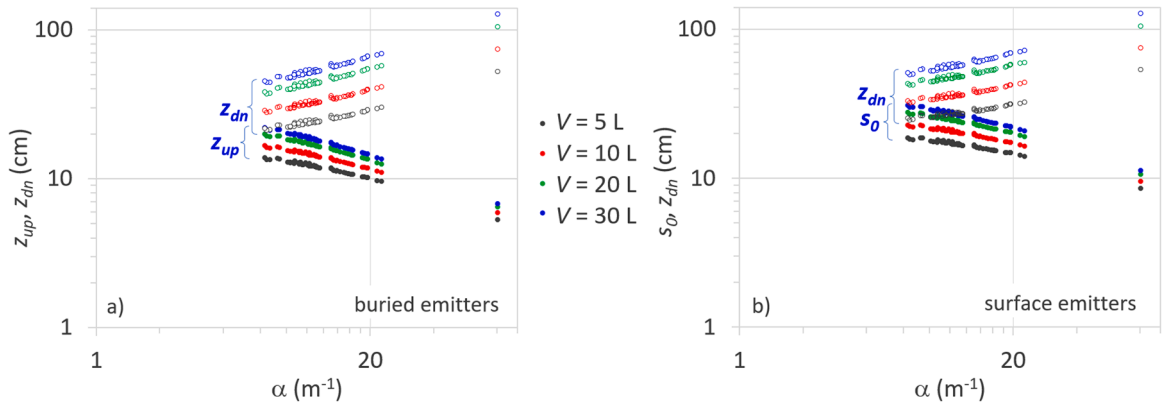

Fig. 4. Relationship between the geometric variables, a) for a buried source and b) for a surface source, versus the α parameter, for different irrigation volumes.

source, $z_{dn} > z_{up}$, while, for a surface source, $z_{dn} > s_0$, indicating an elongated shape of the bulb, which becomes more and more outstretched at increasing α, according to a quite potential power law. Contrarily to z_{dn} that increases with α, z_{up} (Fig. 4a) and s_0 (Fig. 4b) decrease with α, evidencing as obvious that when gravity forces increase as compared with capillarity forces (Reynolds and Elrick, 1991), the bulb expansion upwards for buried sources and laterally for surface sources tends to be limited. Of course, the bulb expansion increases at increasing the irrigation volume, and a quite similar power law shape is maintained.

In Fig. 4, it is also interesting to observe that for any fixed α, by varying V, for both buried and surface sources, the range of variability of z_{dn} is higher than that of s_0 and z_{up}, respectively. Only in the first stages of irrigation (low V and low α), the bulb shape is more spherical than stretched down, while the opposite result is obtained for high V.

To compare the total bulb vertical length of buried and surface sources, the dimensionless ratio between the sum $z_{up} + z_{dn}$ for buried source, $(z_{up} + z_{dn})_{buried}$, and z_{dn} for surface source $(z_{dn})_{surface}$ was evaluated for the entire data set, by imposing different irrigation volumes.

Fig. 5a shows the ratio $(z_{up} + z_{dn})_{buried}/(z_{dn})_{surface}$ versus α for different V. The total bulb vertical length $(z_{up} + z_{dn})_{buried}$ results higher than $(z_{dn})_{surface}$ indicating the advantages in water saving due to adopting subsurface irrigation where buried emitters also wet the soil upwards. However, this benefit tends to vanish at increasing α (Fig. 5a) achieving $(z_{up} + z_{dn})_{buried}$ values close to $(z_{dn})_{surface}$, and more and more as the irrigation volume increases. For any α, the benefit appears more relevant in the first stages of the irrigation, that is when small water volumes have been supplied.

For surface sources, the bulb shape index $(z_{dn})_{surface}/(s_0)_{surface}$ was also considered (Fig. 5b). In this case, the bulb shape index follows an increasing quadratic function of α. Furthermore, the increasing irrigation volume provides higher bulb shape index, since during irrigation the bulb elongates downward more and more.

From an irrigation system design point of view, it is important to predict the vertical length of the bulb by imposing adequate irrigation times and, importantly, by accounting for the spatial variability of soil hydraulic characteristics that have been displayed in Fig. 2. Indeed, watering times that go on longer than necessary determine water waste since the bulb size may overpass the root zone.

For each soil sampling point, the geometric variables are plotted against the irrigation volume in Fig. 6a (for the buried sources) and in Fig. 6b (for the surface source). Except for the α outlier, the curves lay within a bound with an increasing width for larger irrigation volumes. The range of variability of the geometric variables is similar for both buried and surface sources but a bit narrower bound width can be observed for surface emitters than for buried emitters. Contrarily, the geometric bulb variables corresponding to the α outlier determine very different geometric variables compared to the other values. This result means that an uncommonly large α value may provide a high z_{dn} value and hence it could imply underwatering in the root zone.

To evaluate the impact of α in estimating the irrigation volume required to achieve an imposed root depth, applications were performed for the minimum and the maximum α values retrieved in the dataset (6 and 81 m^{-1}) for a buried source. First Eq. (19) was needed to be used for determining the z_{dn} and z_{up} relationship. For the above-mentioned extreme α values, Fig. 7 shows the increasing relationship between $(z_{dn})_{buried}$ and $(z_{up})_{buried}$, and the important effect of α. In particular, Fig. 7 illustrates that for a fixed z_{dn}, e.g. 10 cm, $z_{up} = 2.5$ cm occurs for α =

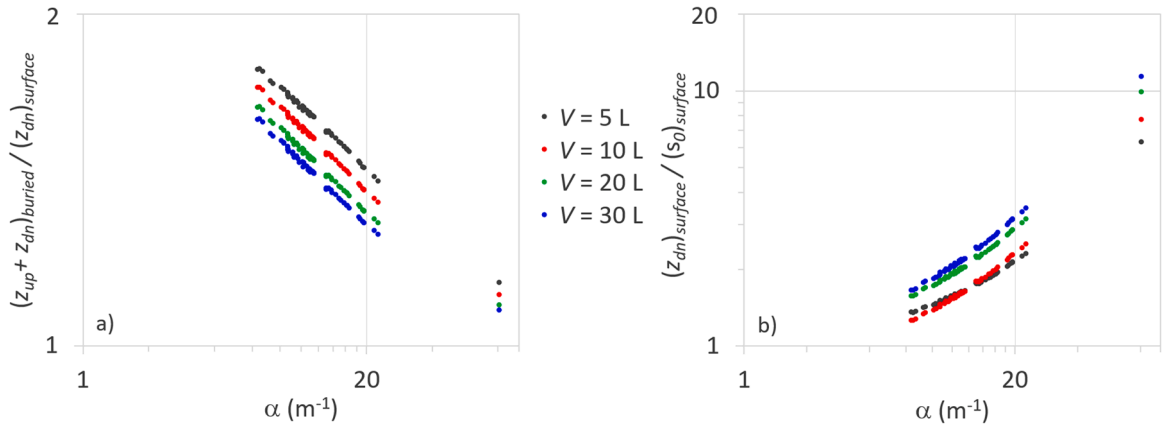

Fig. 5. Relationship between a) the dimensionless $(z_{up} + z_{dn})_{buried}/(z_{dn})_{surface}$ ratio and b) the bulb shape index $(z_{dn})_{surface}/(s_0)_{surface}$, versus the α parameter, for different irrigation volumes.

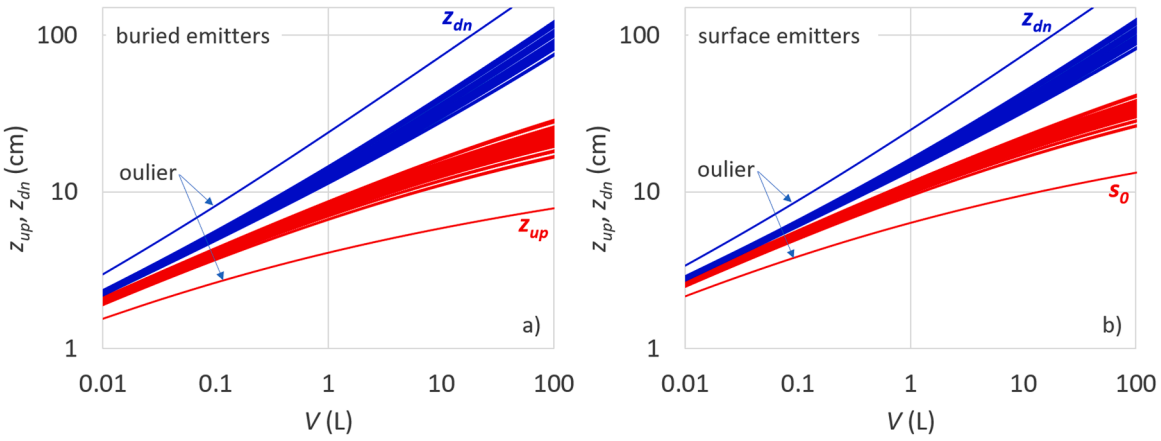

Fig. 6. Geometric bulb variables a) for a buried sources and b) for a surface source, versus the irrigation volume, *V*, for the 56 experimental runs. The geometric bulb variables corresponding to the α outlier is also indicated.

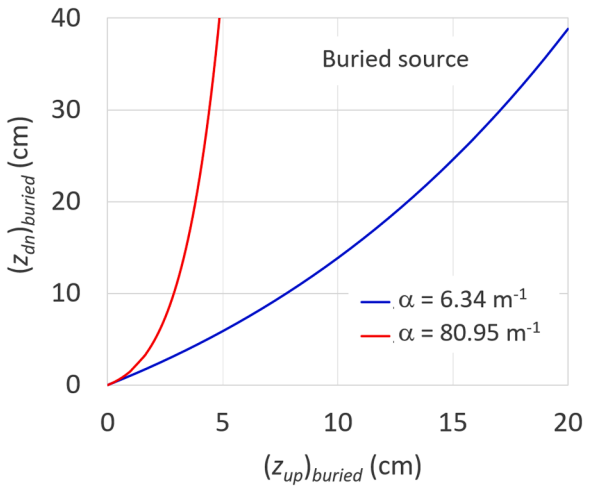

Fig. 7. For a buried source, relationship between z_{dn} and z_{up}, for the minimum $\alpha = 6\ m^{-1}$ and the maximum $\alpha = 81\ m^{-1}$.

81 m^{-1}, while, z_{up} is three times higher (7.5 cm), for $\alpha = 6\ m^{-1}$, and the relationship between z_{dn} and z_{up} is independent by the Δθ value.

For the pairs (z_{dn}, z_{up}) obtained by using Eq. (19), the irrigation volume required to achieve an imposed root depth was determined by Eq. (14) (or by Eq. 15). Fig. 8 plots the irrigation volumes required to achieve an assigned vertical bulb length for both a buried source, $(z_{up} + z_{dn})_{buried}$, and for a surface source (Eq. 20), and both for $\alpha = 6\ m^{-1}$ (Fig. 8a) and for $\alpha = 81\ m^{-1}$ (Fig. 8b).

The comparison between Fig. 8a and Fig. 8b makes it evident the important effect of α value when the desired water irrigation volume is established. Indeed, for fixed values of $(z_{dn} + z_{up})_{buried} = (z_{dn})_{surface}$ equal to 30 cm and 50 cm, indicated by dots in Fig. 8 and reported in Table 3, it can be observed that for the highest α value, irrigation volumes much lower than those for the lowest α value are required to cover the imposed vertical bulb length. In terms of water saving, the benefit of subsurface drip irrigation can be observed for both α values, requiring less water volumes for buried sources than for surface sources, with a lesser extent for the highest α value.

This is because, in soils characterized by high α values, gravity forces

Table 3
Irrigation volumes, V (L), required to achieve bulb vertical lengths equal to 30 cm and to 50 cm, for buried and surface emitters.

Bulb vertical length (cm)	Soil parameters			Buried emitters		Surface emitters	
	α (m^{-1})		z_{up} (cm)	z_{dn} (cm)	V (L)	z_{dn} (cm)	V (L)
30	MIN	6	12.1	17.9	3.1	30	7.9
	MAX	81	4.2	25.8	1.2		1.5
50	MIN	6	17.8	32.2	13.4	50	28.9
	MAX	81	5.1	44.9	3.7		4.4

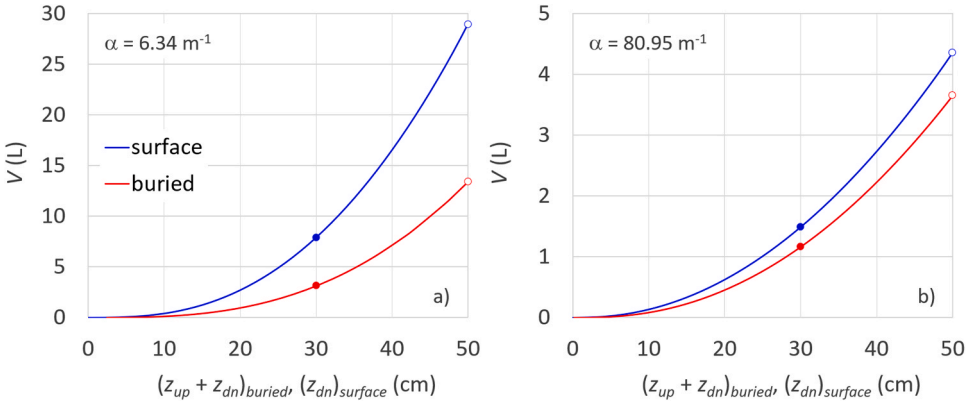

Fig. 8. Irrigation volumes required to achieve an assigned vertical bulb length for a buried source, $(z_{up} + z_{dn})_{buried}$, and for a surface source $(z_{dn})_{surface}$, a) for the minimum value of α (6 m^{-1}) and b) for the maximum value of α (81 m^{-1}). The dots indicate the volumes corresponding to 30 cm and 50 cm reported in Table 3.

play a predominant role compared to capillarity, therefore the bulb takes on a more elongated shape. While in soils characterized by low values of α capillary forces dominate the flow and the bulb shape is more spherical. However, in heterogeneous soils, for a correct design and management of the irrigation system, an adequate determination of the variability of the α parameter is even more necessary because water irrigation volumes established by only considering the highest or the lowest α value could penalize both extreme conditions, and a frequency analysis would be suggested, especially for high spatial variability.

The results obtained in this study demonstrate that the total thickness of the wetted soil layer is highly affected by the soil hydraulic characteristics. The detection of the latter has important implications in irrigation scheduling since irrigation volumes less or greater than those determined by the suggested procedure may determine underwatering or overwatering respectively. In the first case, the root development will be confined in between a thinner depth than that established for the crop, in the second case irrigation water is wasted.

In consideration of the above, predicting the variability in bulb expansion resulting from different soil hydraulic properties is essential to estimate the wetting patterns in trickle irrigation systems. Therefore, this proposed approach represents a valuable and straightforward method for designing more efficient irrigation systems that can contribute to water conservation in a context of water resource scarcity.

5. Conclusions

In this study, a wide dataset of the soil hydraulic properties measured for a sandy-loam to loam soil was used to investigate the impact of their variability in predicting the bulb size for surface and buried emitters. To analyse the bulb size, the solutions provided by Philip's (1984) model were reformulated in dimensional terms and were applied to the above dataset. The results showed that hydraulic properties influenced the geometric variables of the bulb with a similar variability range both for buried and surface sources. In terms of water management, buried source always allows water saving compared to surface source. However, in soils characterized by the highest values of α this benefit is less accentuated due to the downward vertical bulb expansion. Due to the spatial variability of the soil hydraulic properties, which highly impacts the bulb size, more accurate design procedures should be developed, avoiding to only characterize the soil in rough terms such as based on its textural characteristics. In other terms, the methodology applied in this investigation helps include the hydrological behaviour of the soil, which has to affect the emitters' position in the design choice, also considering the crop root distribution. A forward step of the analysis could be establishing a link between the hydrological properties and the design variables. Likely, a development of the design procedure should include some kind of probabilistic analysis of the individually wetted soil volumes. This approach could help to consider, and hence to minimize, the risks of an improper design and management of the irrigation apparatus since uncontrolled irrigation duration can cause the bulb vertical length to go beyond the root zone, thus wasting irrigation water.

CRediT authorship contribution statement

Giorgio Baiamonte: Writing – review & editing, Writing – original draft, Visualization, Validation, Supervision, Methodology, Investigation, Formal analysis, Data curation, Conceptualization. **Vincenzo Alagna:** Writing – review & editing, Data curation. **Samuel Palermo:** Writing – review & editing, Writing – original draft, Visualization, Data curation. **Girolamo Vaccaro:** Writing – review & editing, Data curation. **Dario Autovino:** Writing – review & editing, Writing – original draft. **Massimo Iovino:** Writing – review & editing. **Vincenzo Bagarello:** Writing – review & editing, Writing – original draft, Methodology, Data curation, Conceptualization.

Declaration of Competing Interest

The authors declare that they have no known competing financial interests or personal relationships that could have appeared to influence the work reported in this paper.

Data availability

Data will be made available on request.

Acknowledgements

This work was supported by the European Union – FESR or FSE, PON Research and Innovation 2014–2020 – DM 1062/202.

References

Agosta, M., Alagna, V., Bagarello, V., Caltabellotta, G., Iovino, M., Vaccaro, G., 2023. Hydrodynamic response of a loam soil after wetting with different methods. J. Hydrol. 623, 129770 https://doi.org/10.1016/j.jhydrol.2023.129770.

Al-Ogaidi, A.A.M., Wayayok, A., Rowshon, M.K., Abdullah, A.F., 2016. Wetting patterns estimation under drip irrigation systems using an enhanced empirical model. Agric. Water Manag. 176, 203–213. https://doi.org/10.1016/j.agwat.2016.06.002.

Angulo-Jaramillo, R., Bagarello, V., Di Prima, S., Gosset, A., Iovino, M., Lassabatere, L., 2019. Beerkan Estimation of Soil Transfer parameters (BEST) across soils and scales. J. Hydrol. 576, 239–261. https://doi.org/10.1016/j.jhydrol.2019.06.007.

Autovino, D., Provenzano, G., Monserrat, J., Cots, L., Barragán, J., 2016. Determining optimal seasonal irrigation depth based on field irrigation uniformity and economic evaluations: application for onion crop. J. Irrig. Drain. E-ASCE 142 (10). https://doi.org/10.1061/(ASCE)IR.1943-4774.0001048.

Ayers, R.S., Westcot, D.W., 1985. Water Quality for Agriculture. FAO of the United Nations, Rome, Italy.

Bagarello, V., Caltabellotta, G., Concialdi, P., Iovino, M., 2023. Comparing two methods to perform a beerkan infiltration run in a loam soil at different dates. J. Hydrol. 617, 129095 https://doi.org/10.1016/j.jhydrol.2023.129095.

Bagarello, V., Castellini, M., Di Prima, S., Iovino, M., 2014. Soil hydraulic properties determined by infiltration experiments and different heights of water pouring. Geoderma 213, 492–501. https://doi.org/10.1016/j.geoderma.2013.08.032.

Baiamonte, G., 2016. Simple relationships for the optimal design of paired drip laterals on uniform slopes. J. Irrig. Drain. E-ASCE 142 (2), 04015054. Doi: 10.1061/(ASCE)IR.1943-4774.0000971.

Baiamonte, G., Agnese, C., Singh, V.P., 2023. Multiple Non-linear Reservoirs to Model Water Balance Components in Sandy Soils. In: Sherif, M., Singh, V.P., Sefelnasr, A., Abrar, M. (Eds.), Water Resources Management and Sustainability. Water Science and Technology Library. Springer, Cham. https://doi.org/10.1007/978-3-031-24506-0_3.

Barragan, J., Cots, Ll, Monserrat, J., Lopez, R., Wu, I.P., 2010. Water distribution uniformity and scheduling in micro-irrigation systems for water saving and environmental protection. Biosyst. Eng. 107 (3), 202–211. https://doi.org/10.1016/j.biosystemseng.2010.07.009.

Broadbridge, P., Daly, E., Goard, J., 2017. Exact solutions of the Richards equation with nonlinear plant-root extraction. Water Resour. Res. 53 (11), 9679–9691. https://doi.org/10.1002/2017WR021097.

Cook, F.J., Thorburn, P.J., Fitch, P., Bristow, K.L., 2003. WetUp: A software tool to display approximate wetting patterns from drippers. Irrig. Sci. 22, 129–134. https://doi.org/10.1007/s00271-003-0078-2.

Das Gupta, S., Mohanty, B.P., Köhne, J.M., 2006. Soil Hydraulic Conductivities and their Spatial and Temporal Variations in a Vertisol. Soil Sci. Soc. Am. J. 70 (6), 1872–1881. https://doi.org/10.2136/sssaj2006.0201.

Di Prima, S., Stewart, R.D., Castellini, M., Bagarello, V., Abou Najm, M.R., Pirastru, M., Giadrossich, F., Iovino, M., Angulo-Jaramillo, R., Lassabatere, L., 2020. Estimating the macroscopic capillary length from Beerkan infiltration experiments and its impact on saturated soil hydraulic conductivity predictions. J. Hydrol. 589, 125159 https://doi.org/10.1016/j.jhydrol.2020.125159.

Elrick, D.E., Reynolds, W.D., 1992. Methods for analyzing constant-head well permeameter data. Soil Sci. Soc. Am. J. 56 (1), 320–323. https://doi.org/10.2136/sssaj1992.03615995005600010052x.

Fernández-Gálvez, J., Simmonds, L.P., 2006. Monitoring and modelling the three-dimensional flow of water under drip irrigation. Agric. Water Manag. 83 (3), 197–208. https://doi.org/10.1016/j.agwat.2005.11.008.

Gardner, W.R., 1958. Some steady-state solutions of the unsaturated moisture flow equation with application to evaporation from a water table. Soil Sci. 85 (4), 228–232. https://doi.org/10.1097/00010694-195804000-00006.

Glantz, S.A., 2012. Primer of Biostatistics. McGraw-Hill, New York.

{C}Goyal, M.R.{C} 2014. Sustainable micro irrigation: Principles and practices. New York. https://doi.org/10.1201/b17155.

Haverkamp, R., Ross, P.J., Smettem, K.R.J., Parlange, J.Y., 1994. Three-dimensional analysis of infiltration from the disc infiltrometer: 2. Physically based infiltration equation. Water Resour. Res. 30 (11), 2931–2935. https://doi.org/10.1029/94WR01788.

Horton, R.E., 1941. An approach toward a physical interpretation of infiltration-capacity. Soil Sci. Soc. Am. J. 5, 399–417. https://doi.org/10.2136/sssaj1941.03615995000500c0075x.

Kandelous, M.M., Šimůnek, J., 2010a. Comparison of numerical, analytical, and empirical models to estimate wetting patterns for surface and subsurface drip irrigation. Irrig. Sci. 28 (5), 435–444. https://doi.org/10.1007/s00271-009-0205-9.

Kandelous, M.M., Šimůnek, J., 2010b. Numerical simulations of water movement in a subsurface drip irrigation system under field and laboratory conditions using HYDRUS-2D. Agric. Water Manag. 97 (7), 1070–1076. https://doi.org/10.1016/j.agwat.2010.02.012.

Keller, J., Bliesner, R.D., 1990. Sprinkle and Trickle Irrigation. The Blackburn Press, New York, p. 652.

Lafolie, F., Guennelon, R., van Genuchten, M.Th, 1989. Analysis of water flow under trickle irrigation: I. Theory and numerical solution. Soil Sci. Soc. Am. J. 53 (5), 1310–1318. https://doi.org/10.2136/sssaj1989.03615995005300050002x.

Lassabatère, L., Angulo-Jaramillo, R., Soria Ugalde, J.M., Cuenca, R., Braud, I., Haverkamp, R., 2006. Beerkan estimation of soil transfer parameters through infiltration experiments-BEST. Soil Sci. Soc. Am. J. 70 (2), 521–532. https://doi.org/10.2136/sssaj2005.0026.

Lilliefors, H.W., 1967. On the Kolmogorov-Smirnov test for normality with mean and variance unknown. J. Am. Stat. Assoc. 62 (318), 399–402. https://doi.org/10.1080/01621459.1967.10482916.

Lubana, P.P.S., Narda, N.K., 2001. SW-soil and water: modelling soil water dynamics under trickle emitters - a review. J. Agric. Eng. Res. 78 (3), 217–232. https://doi.org/10.1006/jaer.2000.0650.

Lubana, P.P.S., Narda, N.K., Brown, L.C., 2004. Application of a hemispherical model to predict radius of wetted soil volume under point source emitters for trickle irrigated tomatoes in Punjab state, India. ASAE Annual Meeting, 042243. https://doi.org/10.13031/2013.16434.

Mubarak, I., Mailhol, J.C., Angulo-Jaramillo, R., Bouarfa, S., Ruelle, P., 2009. Effect of temporal variability in soil hydraulic properties on simulated water transfer under high-frequency drip irrigation. Agric. Water Manag. 96 (11), 1547–1559. https://doi.org/10.1016/j.agwat.2009.06.011.

Nakayama, F.S., Bucks, D.A., 1986. Trickle Irrigation for Crop Production. Design, Operation and Management. Elsevier, Amsterdam.

Pachepsky, Y., Karahan, G., 2022. On shapes of cumulative infiltration curves. Geoderma 412, 115715. https://doi.org/10.1016/j.geoderma.2022.115715.

Philip, J.R., 1984. Travel times from buried and surface infiltration point sources. Water Resour. Res. 20 (7), 990–994. https://doi.org/10.1029/WR020i007p00990.

Provenzano, G., Alagna, V., Autovino, D., Juarez, J.M., Rallo, G., 2016. Analysis of geometrical relationships and friction losses in small-diameter lay-flat polyethylene pipes. J. Irrig. Drain. E-ASCE 142 (2), 04015041. https://doi.org/10.1061/(ASCE)IR.1943-4774.0000958.

Regalado, C.M., Muñoz-Carpena, R., 2004. Estimating the saturated hydraulic conductivity in a spatially variable soil with different permeameters: a stochastic Kozeny-Carman relation. Soil Tillage Res. 77 (2), 189–202. https://doi.org/10.1016/j.still.2003.12.008.

Revol, P., Clothier, B.E., Mailhol, J.-C., Vachaud, G., Vauclin, M., 1997. Infiltration from a surface point source and drip irrigation: 2. An approximate time-dependent solution for wet-front position. Water Resour. Res. 33 (8), 1869–1874. https://doi.org/10.1029/97WR01007.

Reynolds, W.D., Bowman, B.T., Drury, C.F., Tan, C.S., Lu, X., 2002. Indicators of good soil physical quality: Density and storage parameters. Geoderma 110 (1-2), 131–146. https://doi.org/10.1016/S0016-7061(02)00228-8.

Reynolds, W.D., Elrick, D.E., 1991. Determination of hydraulic conductivity using a tension infiltrometer. Soil Sci. Soc. Am. J. 55 (3), 633–639. https://doi.org/10.2136/sssaj1991.03615995005500030001x.

Richards, L.A., 1931. Capillary conduction of liquids through porous mediums. Physics 1 (5), 318–333. https://doi.org/10.1063/1.1745010.

Singh, D.K., Rajput, T.B.S., Singh, D.K., Sikarwar, H.S., Sahoo, R.N., Ahmad, T., 2006. Simulation of soil wetting pattern with subsurface drip irrigation from line source. Agric. Water Manag. 83 (1–2), 130–134. https://doi.org/10.1016/j.agwat.2005.11.002.

Stewart, R.D., Rupp, D.E., Najm, M.R.A., Selker, J.S., 2013. Modeling effect of initial soil moisture on sorptivity and infiltration. Water Resour. Res. 49 (10), 7037–7047. https://doi.org/10.1002/wrcr.20508.

Subbaiah, R., 2013. A review of models for predicting soil water dynamics during trickle irrigation. Irrig. Sci. 31 (3), 225–258. https://doi.org/10.1007/s00271-011-0309-x.

Thorburn, P.J., Cook, F.J., Bristow, K.L., 2003. Soil-dependent wetting from trickle emitters: Implications for system design and management. Irrig. Sci. 22, 121–127. https://doi.org/10.1007/s00271-003-0077-3.

Warrick, A.W., 1998. Spatial variability, in: Environmental Soil Physics Appendix 1. D. Hillel, California, pp. 665–675.

White, I., Sully, M.J., 1987. Macroscopic and microscopic capillary length and time scales from field infiltration. Water Resour. Res. 23 (8), 1514–1522. https://doi.org/10.1029/WR023i008p01514.

Youngs, E.G., Elrick, D.E., Reynolds, W.D., 1993. Comparison of steady flows from infiltration rings in “Green and Ampt” and “Gardner” soils. Water Resour. Res. 29 (6), 1647–1650. https://doi.org/10.1029/93WR00006.